Realization of Sensory-Based Biped Walking

Hun-ok Lim[⋆†], Yu Ogura[∗] and Atsuo Takanishi[∗†]
[⋆]Department of System Design Engineering, Kanagawa Institute of Technology
1030 Shimoogino, Atsugi, Kanagawa, 243-0292 Japan
Tel/Fax:81-46-291-3266, E-mail: holim@sd.kanagawa-it.ac.jp
[∗]Department of Mechanical Engineering, Waseda University
[†]Humanoid Robotics Institute, Waseda University

Abstract

This paper describes realtime walking based on sensory information. In this study, a biped robot having a trunk is considered. The motion of the trunk balances the whole body of the biped robot while the legs locomotes on the ground. How to calculate the motion of the trunk is proposed using the ZMP concept. Also, an online walking pattern is discussed which is generated in realtime on the basis of walking parameters selected by visual and auditory sensors. In order to realize biped walking, we have constructed a forty-three degrees of freedom biped robot, WABIAN-RV (WAseda BIped humANoid robot-Revised V). Its height is 1.89[m] and its total weight is 131.4[kg]. Various walking experiments using WABIAN-RV are conducted on the plane, and the validity of its mechanism and control is verified.

1. Introduction

Biped humanoid robots are expected to be used not only into industrial areas, but also into non-industrial areas, such as to services in homes and offices and for social welfare. To date, we have studied biped-walking motion with two main thrusts to apply the biped robots to the fields. One thrust has been toward realizing dynamic complete walking on not only even or uneven terrain but also hard or soft terrain. In 1973, we developed WABOT-1 that consists of a torso, a perceptual system and two artificial arms and legs. The biped robot realized the static walking on a horizontal plane [1]. In 1980, we realized the quasi-dynamic complete walking by using WL series. In 1984, the complete dynamic walking with the walking speed 1.3 s/step was realized by using the program control and the sequence control [2]. In addition, the dynamic walking on the uneven terrain like stairs and inclined planes was realized by modifying a preset walking pattern. The other thrust has been toward exploring robot-environment interaction and human emotion. The dynamic biped walking was achieved under the unknown external forces applied by an environment in 1989 [3]. Also, the emotional motion of the biped robot was presented in 1999, which is expressed by the parameterization of its body motion [4].

In order to realize advanced biped walking in human living/working environments, we should employ the technologies of human-robot interaction [5, 6, 7, 8, 9, 10]. Also, human safety should be considered in developing humanoid robots [11, 12]. However, there are few reports on the realization of follow walking under physical interaction between a human and a biped walking robot based on various action models [13]. It is difficult for the biped robot to achieve various interactive walking due to the stability. Therefore, a compensatory control method is discussed in this paper, which can cancel moments generated by the motion of the lower-limbs. For biped locomotion, a complete online walking pattern that is generated on the basis of walking parameters is also described.

This paper is organized as follows. Section 2 describes a compensatory body motion to cancel moments generated by the motion of the lower-limbs. Section 3 describes an online walking pattern generation. Section 4 illustrates an experimental system and shows experimental results. Finally, Section 5 provides conclusions.

2. Compensatory Body Motion

To achieve biped walking, the functional roll of parts of the biped humanoid robot should be divided. The lower-limbs should be able to adapt to terrain, while the upper-body should be able to maintain stability. In this section, how to get the motion of the trunk and the waist is described

2.1 Coordinate Frames

A 43-DOF biped model with rotational joints is considered in this study, which consists of two 6-DOF legs, two 7-DOF arms, two 3-DOF hands, a 4-DOF neck, two 2-DOF eyes and a torso with a 3-DOF waist. To define mathematical quantities, a world coordinate frame $\mathcal{F}$ is fixed on the floor where the biped robot can walk and a moving coordinate frame $\bar{\mathcal{F}}$ is attached on the center of the waist to consider the relative motion of each particle (see Figure 1). In modeling, five assumptions are defined as follows:
(1) the biped robot consists of a set of particles,
(2) the foothold of the biped robot is rigid and not moved by any force and moment,
(3) the contact region between the foot and the floor surface is a set of contact points,
(4) the coefficients of friction for rotation around the X, Y and Z-axes are nearly zero at the contact point between the feet and the floor surface and
(5) the feet of the robot do not slide on the contact surface.

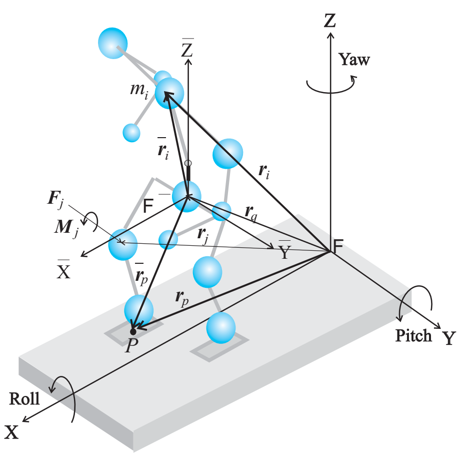

Figure 1: Coordinate frames

2.2 ZMP Equation

Under the modeling assumptions, the moment balance around a contact point p between the foot and the ground with respect to the world coordinate frame can be written as

$$\sum_{j=1}^{n}((\boldsymbol{r}_j - \boldsymbol{r}_p) \times \boldsymbol{F}_j + \boldsymbol{M}_j) - \sum_{i=1}^{n} m_i(\boldsymbol{r}_i - \boldsymbol{r}_p) \times (\ddot{\boldsymbol{r}}_i + \boldsymbol{G}) = \boldsymbol{T} \quad (1)$$

where $\boldsymbol{r}_p$ is the position vector of the point p from the origin of $\mathcal{F}$. m_i is the mass of the particle i. $\boldsymbol{r}_i$ and $\ddot{\boldsymbol{r}}_i$ denote the position and acceleration vectors of the particle i with respect to the world coordinate frame $\mathcal{F}$, respectively. $\boldsymbol{G}$ is the gravitational acceleration vector. $\boldsymbol{T}$ is the moment vector acting on the contact point p. $\boldsymbol{r}_j$ denotes the position vector of the particle j with respect to the world coordinate frame $\mathcal{F}$. $\boldsymbol{F}_j$ and $\boldsymbol{M}_j$ denote the force and the moment vectors acting on the particle j relative to the frame $\mathcal{F}$, respectively.

Let ZMP be on the point p. The moment $\boldsymbol{T}$ is zero according to the ZMP concept. To get the relative motion of particles, Equation (1) is changed relative to the moving frame $\bar{\mathcal{F}}$ as follows:

$$\sum_{i=1}^{n} m_i(\bar{\boldsymbol{r}}_i - \bar{\boldsymbol{r}}_{zmp}) \times (\ddot{\bar{\boldsymbol{r}}}_i + \ddot{\boldsymbol{r}}_q + \boldsymbol{G} + \dot{\bar{\boldsymbol{\omega}}} \times \bar{\boldsymbol{r}}_i + 2\bar{\boldsymbol{\omega}} \times \dot{\bar{\boldsymbol{r}}}_i + \bar{\boldsymbol{\omega}} \times (\bar{\boldsymbol{\omega}} \times \bar{\boldsymbol{r}}_i)) - \sum_{j=1}^{n}((\bar{\boldsymbol{r}}_j - \bar{\boldsymbol{r}}_{zmp}) \times \bar{\boldsymbol{F}}_j + \bar{\boldsymbol{M}}_j) = \boldsymbol{0}, \quad (2)$$

where $\bar{\boldsymbol{r}}_{zmp}$ is the position vector of ZMP with respect to the $\bar{\mathcal{F}}$. $\boldsymbol{r}_q$ is the position vector of the origin of the frame $\bar{\mathcal{F}}$ from the origin of the frame $\mathcal{F}$. $\bar{\boldsymbol{\omega}}$ and $\dot{\bar{\boldsymbol{\omega}}}$ denote the angular velocity and acceleration vectors, respectively.

Equation (2) is non-linear because the three-axis motion of the trunk is interferential each other. It, therefore, is difficult to derive analytic solutions of the trunk and the waist. We assume that (a) the external forces are not considered in the approximate model, (b) the upper body is modeled as a four-mass model, (c) the moving frame does not rotate, (d) the trunk and the waist do not move vertically, and (e) the trunk arm rotates on the horizontal plane only.

In case that the moments are not generated by the fictitious forces, the moment $\boldsymbol{M}$ generated by the lower-limb's motion, $\boldsymbol{M} = [M_x \; M_y \; M_z]^T$, can be divided as three components as follows:

$$-m_t(\bar{z}_t - \bar{z}_{zmp})(\ddot{\bar{x}}_t + \ddot{\bar{x}}_q) - m_t g_z(\bar{x}_t - \bar{x}_{zmp}) - m_w(\bar{z}_w - \bar{z}_{zmp})(\ddot{\bar{x}}_w + \ddot{\bar{x}}_q) - m_w g_z(\bar{x}_w - \bar{x}_{zmp}) = M_y, \quad (3)$$

$$m_t(\bar{z}_t - \bar{z}_{zmp})(\ddot{\bar{y}}_t + \ddot{\bar{y}}_q) + m_t g_z(\bar{y}_t - \bar{y}_{zmp})$$

$$+m_w(\bar{z}_w - \bar{z}_{zmp})(\ddot{\bar{y}}_w + \ddot{\bar{y}}_q) + m_w g_z(\bar{y}_w - \bar{y}_{zmp}) = M_x, \quad (4)$$

$$-m_s l^2(\ddot{\theta}_t + \dot{\omega}) - m_t(\bar{x}_t - \bar{x}_{zmp})(\ddot{\bar{y}}_t + \ddot{\bar{y}}_q) + m_t(\bar{y}_t - \bar{y}_{zmp})(\ddot{\bar{x}}_t + \ddot{\bar{x}}_q) - m_w(\bar{x}_w - \bar{x}_{zmp})(\ddot{\bar{y}}_w + \ddot{\bar{y}}_q) + m_w(\bar{y}_w - \bar{y}_{zmp})(\ddot{\bar{x}}_w + \ddot{\bar{x}}_q) = M_z, \quad (5)$$

where m_s denotes the mass of both shoulders including the mass of the arms. m_t is the mass of the torso including the head, shoulders and arms, and m_w is the mass of the waist. $\bar{\boldsymbol{r}}_t = [\bar{x}_t\ \bar{y}_t\ \bar{z}_t]^T$ and $\bar{\boldsymbol{r}}_w = [\bar{x}_w\ \bar{y}_w\ \bar{z}_w]^T$ are the position vectors of the neck and the waist with respect to the $\bar{\mathcal{F}}$, respectively. $\bar{\boldsymbol{r}}_s = [\bar{x}_s\ \bar{y}_s\ \bar{z}_s]^T$ is the shoulder position vector with respect to the neck frame. θ_t is the vertical angle of the trunk. l is the length between the neck and the shoulder.

M_x, M_y, M_z are periodic functions because each particle of the lower-limbs and the time trajectory of ZMP move periodically with respect to the moving frame $\bar{\mathcal{F}}$. Therefore, each equation can be represented as a Fourier series. Comparing the Fourier transform coefficients of both sides of each equation, the approximate periodic solutions of the pitch and the roll trunk and waist can be obtained. By regarding a complete walking as one walking cycle and making static standing states before and after walking long enough, the approximate solutions of the compensatory trunk and waist for the complete walking can be derived. Also, the strict solutions of the trunk and the waist motion can be obtained by a recursive method.

3. Complete Walking Pattern Generation

A walking cycle consists of five phases as shown in Figure 2: stationary, transient, steady, trtansient and stationary phases. The transient phase is a step after or before the stationary phase because the dynamics of the upper-body should be considered for stability. An online pattern generator makes a continuous walking pattern as shown in Figure 3. First, walking parameters are inputted to the pattern generator according to the visual and auditory information and so on, which are a step length, step height and step direction. Second, the pattern generator makes a five-step pattern of the lower-limbs and sets a target ZMP pattern in the stable polygon. Third, the compensatory motion of the trunk and the waist is calculated from the trajectories of the lower-limbs and the ZMP by using a walking motion control method. Finally, the middle step of the five-step pattern and the compensatory motion pattern is selected for a next step and is returned to the first step of the pattern generator to make a future step.

We here describe how to determine the pattern of the lower-limb more in detail as follows: (a) Five steps are made in realtime when the biped humanoid robot starts, which are composed of four-transient steps and a steady step. The pattern generator selects from the first step to the third step. (b) On the third step, three steps (from the fourth step to the fifth step) are generated to satisfy the conditions of the second and the third lower-limb step. The fourth step is chosen. (c) On the fourth step, three steps (from the fifth step to the seventh step) are generated to satisfy the conditions of the third and the fourth lower-limb step. The fifth, sixth and seventh step are selected. (d) A continuous walking pattern is generated in realtime to repeat the above procedure. Figure 4 shows the pattern generation of the lower-limb.

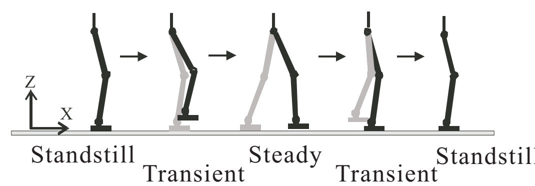

Figure 2: A walking cycle

4. Experiments

Various walking experiments are conducted to confirm the validity of the walking mechanism and the compensatory motion control. In this section, the experimental systems are described briefly, and the experimental results are presented.

4.1 System Description

To explore follow-walking motion, a forty-three mechanical degrees of freedom WABIAN-RV with a human configuration has been constructed as shown in Figure 5. The height of the WABIAN-RV is about 1.89 m and its total weight is 131.4 kg.

Duralumin, GIGAS (YKK Corporation) and CFRP (Carbon Fiber Reinforced Plastic) are mainly employed as structural materials of the WABIAN-RV. The body and legs are driven by AC servo motors with reduction gears. The neck, hands and arms are

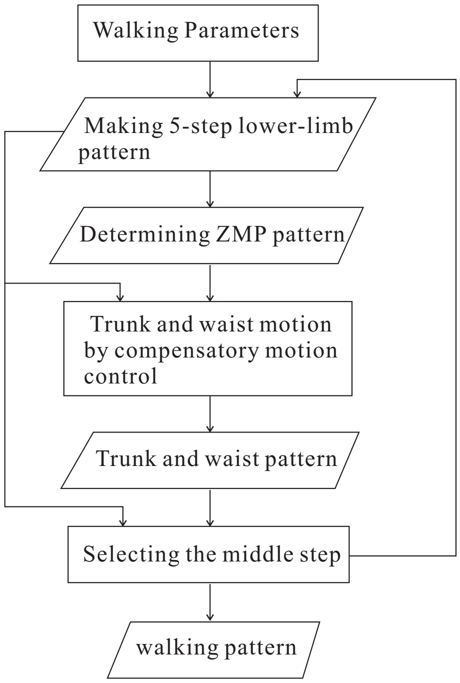

Figure 3: Online pattern generation

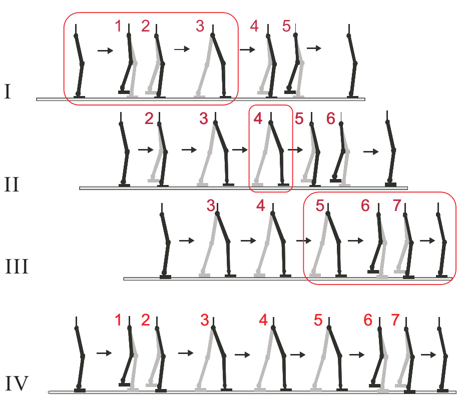

Figure 4: Lower-limb's pattern generation

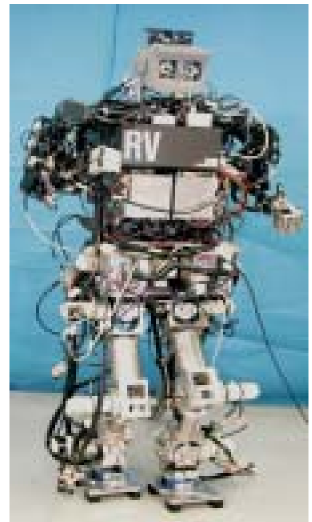

Figure 5: Photo of the WABIAN-RV.

actuated by DC servo motors with reduction gears, but the eyes by DC servo motors without reduction gears. Two CCD cameras are used to recognize the walking direction, which is attached on the head.

4.2 Visual System

The visual system of WABIAN-RV is designed to mimic some of the capabilities of the human visual system. Two tracking visions are used to sense three-dimensional information. The realtime walking pattern generation is experimented on the basis of visual information as follow. (1) Before walking, the tracking visions are initialized, and both hands of a human are specified as tracking points. (2) To know simply the walking direction, gesture recognition is conducted by one eye. Suppose that two points tracked by one eye are the points tracked by the right and the left eye, respectively. According to the distance between two points, the forth and the back direction are defined. The differences of right and left initial and measured values, dP_r and dP_l, can be obtained as

$$dP_r = P_r - P_{r0},$$
$$dp_l = P_l - P_{l0}, \quad (6)$$

where P_{r0} and P_{l0} denote the right and the left initial tracking points, respectively. P_r and P_l are the right and the left current tracking point, respectively.

The step length of forth-and-back and righ-and-back walking, S_{fb} and S_{rf} is described as

$$S_{fb} = K_{fb}(dP_r - dP_l),$$

$$S_{rf} = K_{rf}\frac{(dP_r - dP_l)}{2}, \quad (7)$$

where K_{fb} and K_{rf} are the gains of forth-and-back and right-and-left walking, respectively. In this experiments, K_{fb} and K_{rf} are set as 0.001, respectively.

(3) A walking pattern is determined by the online pattern generator based on the visual information.

4.3 Auditory System

IMB's ViaVoice system is used as a voice recognition engine. In this study, we make the system recognize preset voices only. The step length is defined by compiling the text file of Grammar Control. Table 1 shows the step length with regard to specialized vocabularies.

Table 1: Voice Command.

Voice	SP m	LP m	Turnning deg
Forward	0.10	0.00	0.00
Backward	-0.10	0.00	0.00
Right	0.00	-0.05	0.00
Left	0.00	0.05	0.00
Right turnning	0.00	0.00	-5.00
Left Turning	0.00	0.00	5.00
Standstill	0.00	0.00	0.00
Stop	0.00	0.00	0.00

SP: Sagittal Plane
LP: Lateral Plane

4.4 Experimental Results

In realtime walking experiments using the visual system, continuous dynamic walking on a flat plane is realized with the step time of 1.12 s/step, the forth-and-back step length of 0.1 m/step, the side step length of 0.05 m/step. Figure 6 show a scene of the walking experiment conducted by the visual sense. Also, continuous dynamic walking on a flat plane using voice recognition is realized with the step time of 0.96 s/step, the forth-and-back step length of 0.1 m/step, the side step length of 0.05 m/step and the turning angle of 5 deg/step. Figure 7 shows a scene of the walking experiment conducted by the auditory sense.

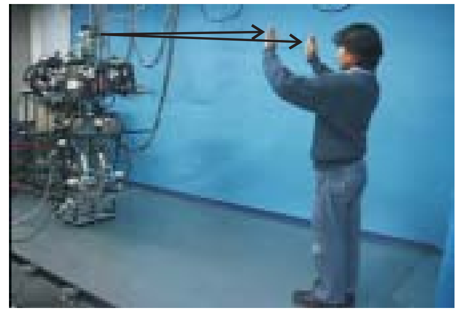

Figure 6: Walking experiment by visual tracking

5. Conclusion

A compensatory control method was presented to achieve interactive walking. Using the control method, the motion of the trunk and waist is calculated which compensates for moments generated by the motion of the lower-limbs, upper-limbs and head. A complete walking pattern generation is also described for biped locomotion. To confirm the control method, we have developed a human-like biped walking robot, WABIAN-RV. Using the biped robot and sensory systems, various realtime walking experiments are conducted, and the effectiveness of the control method and the hardware was confirmed.

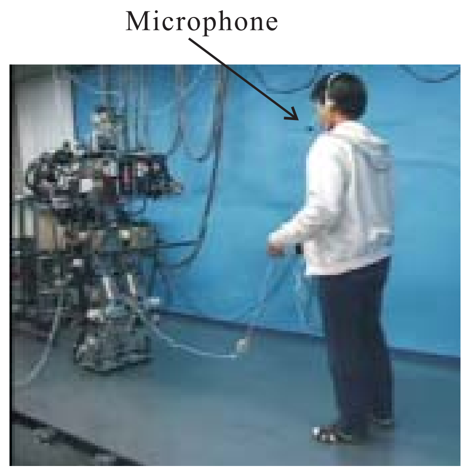

Figure 7: Walking experiment by voice

Acknowledgment

This study has been conducted as a part of the humanoid project at Humanoid Robotics Institute, Waseda University. This study was funded in part by JSPS (Japan Society for the Promotion of Science) under Japanese Grant-in-Aid for Scientific Research and NEDO (New Energy and Industrial Technology

Development Organization). The authors would like to thank Okino Industries Ltd., Harmonic Drive Systems Inc. and YKK Corporation for supporting us in developing the hardware.

References

[1] I. Kato, S. Ohteru, H. Kobayashi, K. Shirai, and A. Uchiyama, "Information-power machine with senses and limbs," in *Proc. CISM-IFToMM Symp. Theory and Practice of Robots and Manipulators*, Udine, Italy, Sep. 1973, pp. 12–24.

[2] A. Takanishi, M. Ishida, Y. Yamazaki, and I. Kato, "The realization of dynamic walking by the biped walking robot," in *Proc. IEEE Int. Conf. Robotics and Automation*, St. Louis, MO, Mar. 1985, pp. 459–466.

[3] A. Takanishi, T. Takeya, H. Karaki, M. Kumeta, and I. Kato, "A control method for dynamic walking under unknown external force," in *Proc. IEEE/RSJ Int. Workshop Intelligent Robots and Systems*, Tsuchiura, Japan, Jul. 1990, pp. 795–801.

[4] H. O. Lim, A. Ishii, and A. Takanishi, "Motion pattern generation for emotion expression," in *Proc. Int. Symp. Humanoid Robots*, Tokyo, Japan, Oct. 1999, pp. 36–41.

[5] I. D. Walker, "The use of kinematic redundancy in reducing impact and contact effects in manipulation," in *Proc. IEEE Int. Conf. Robotics and Automation*, Cincinnati, OH, May 1990, pp. 434–446.

[6] K. Kitagaki and M. Uchiyama, "Optimal approach velocity of end-effector to the environment," in *Proc. IEEE Int. Conf. Robotics and Automation*, Nice, France, May 1992, pp. 1928–1934.

[7] R. Volpe and P. Khosla, "Experimental verification of a strategy for impact control," in *Proc. IEEE Int. Conf. Robotics and Automation*, Sacramento, CA, Apr. 1991, pp. 1854–1860.

[8] O. Khatib, K. Yokoi, K. Chang, D. Ruspini, R. Holmberg, A. Casal, and A. Baader, "Force strategy for cooperative tasks in multiple mobile manipulation systems," in *Preprints of the 7th Int. Symp. Robotics research*, Munich, Germany, 1995, pp. 299–307.

[9] M. T. Mason, "Compliance and force control for computer controlled manipulators," *IEEE Trans. Systems, Man, and Cybernetics*, vol. 11, no. 6, pp. 418–432, Jun. 1981.

[10] M. Koga, K. Kosuge, K. Furuta, and K. Nosaki, "Coordinated motion control of robot arms based on the virtual internal model," *IEEE Trans. Robotics and Automation*, vol. 8, no. 1, pp. 77–85, Feb. 1992.

[11] H. O. Lim and K. Tanie, "Collision-tolerant control of human friendly robot with viscoelastic trunk," *IEEE/ASME Trans. on Mechatronics*, vol. 4, no. 4, pp. 417–427, Dec. 1999.

[12] T. Morita, K. Shibuya, and S. Sugano, "Design and control of mobile manipulation system for human symbiotic humanoid: Hadaly-2," in *Proc. IEEE Int. Conf. Robotics and Automation*, Leuven, Belgium, May 1998, pp. 1315–1320.

[13] S. Setiawan, S. Hyon, J. Yamaguchi, and A. Takanishi, "Physical interaction between human and a bipedal humanoid robot -realization of human-follow walking-," in *Proc. IEEE Int. Conf. Robotics and Automation*, Detroit, Mich., May 1999, pp. 361–367.